

# Localized Induction of the ATP-Binding Cassette B19 Auxin Transporter Enhances Adventitious Root Formation in Arabidopsis<sup>1[C][W][OA]</sup>

Poornima Sukumar<sup>2</sup>, Gregory S. Maloney<sup>2</sup>, and Gloria K. Muday\*

Department of Biology, Wake Forest University, Winston-Salem, North Carolina 27109

ORCID ID: 7003510478 (G.K.M).

Adventitious roots emerge from aerial plant tissues, and the induction of these roots is essential for clonal propagation of agriculturally important plant species. This process has received extensive study in horticultural species but much less focus in genetically tractable model species. We have explored the role of auxin transport in this process in Arabidopsis (*Arabidopsis thaliana*) seedlings in which adventitious root initiation was induced by excising roots from low-light-grown hypocotyls. Inhibition of auxin transport from the shoot apex abolishes adventitious root formation under these conditions. Root excision was accompanied by a rapid increase in radioactive indole-3-acetic acid (IAA) transport and its accumulation in the hypocotyl above the point of excision where adventitious roots emerge. Local increases in auxin-responsive gene expression were also observed above the site of excision using three auxin-responsive reporters. These changes in auxin accumulation preceded cell division events, monitored by a cyclin B1 reporter (pCYCB1;1:GUS), and adventitious root initiation. We examined excision-induced adventitious root formation in auxin influx and efflux mutants, including *auxin insensitive1*, *pin-formed1* (*pin1*), *pin2*, *pin3*, and *pin7*, with the most profound reductions observed in *ATP-binding cassette B19* (*ABCB19*). An *ABCB19* overexpression line forms more adventitious roots than the wild type in intact seedlings. Examination of transcriptional and translational fusions between *ABCB19* and green fluorescent protein indicates that excision locally induced the accumulation of *ABCB19* transcript and protein that is temporally and spatially linked to local IAA accumulation leading to adventitious root formation. These experiments are consistent with localized synthesis of *ABCB19* protein after hypocotyl excision leads to enhanced IAA transport and local IAA accumulation driving adventitious root formation.

The root structure of plants includes a primary root from which lateral roots form and may often include adventitious roots that emerge from aerial tissues. While primary roots are formed during embryogenesis, lateral and adventitious roots are formed post-embryonically (Malamy and Benfey, 1997). Both lateral and adventitious roots function to increase nutrient and water uptake and anchor plants in soil. The ability of stems to initiate adventitious root formation depends on many environmental and physiological factors (De Klerk et al., 1999; Li et al., 2009). Formation of adventitious roots on stem segments is widely

exploited for clonal propagation of important horticultural, crop, and forest species. Hormonal and wounding controls of this process have been described (De Klerk et al., 1999; Abarca and Díaz-Sala, 2009; Li et al., 2009), with the role of auxin transport in adventitious rooting being described in a diversity of species, including pine (*Pinus taeda*; Diaz-Sala et al., 1996; Hutchison et al., 1999), carnation (*Dianthus caryophyllus*; Garrido et al., 2002), and mango (*Mangifera indica*; Li et al., 2012). The molecular mechanisms by which root excision and auxin induce adventitious root formation are not yet clear and would be facilitated by studies in a genetically tractable model species.

It is a common horticultural practice to apply auxin to stem cuttings to increase the initiation and elongation of adventitious roots (De Klerk et al., 1999; Li et al., 2009). Auxin application is also effective in enhancing adventitious root formation in intact hypocotyls of Arabidopsis (*Arabidopsis thaliana*; Sorin et al., 2005; Wilmoth et al., 2005). Several studies indicate that as Arabidopsis hypocotyls mature, the induction of adventitious root formation by excision or auxin is reduced, consistent with a developmental context for this process (Díaz-Sala et al., 2002; Correa et al., 2012). In addition, two Arabidopsis mutants that have endogenously high levels of indole-3-acetic acid (IAA), *superroot* (*sur*) and *rooty*, exhibit a proliferation of adventitious roots (Boerjan et al., 1995; Celenza et al.,

<sup>1</sup> This work was supported by the U.S. Department of Agriculture National Institute of Food and Agriculture program (2009–65116–20436 to G.K.M.) and the National Science Foundation Major Research Instrumentation Program (grant nos. NSF–DBI 0500702, MRI–0722926, and MRI–1039755).

<sup>2</sup> These authors contributed equally to the article.

\* Corresponding author; e-mail muday@wfu.edu.

The author responsible for distribution of materials integral to the findings presented in this article in accordance with the policy described in the Instructions for Authors (<http://www.plantphysiol.org>) is: Gloria K. Muday (muday@wfu.edu).

[C] Some figures in this article are displayed in color online but in black and white in the print edition.

[W] The online version of this article contains Web-only data.

[OA] Open Access articles can be viewed online without a subscription.

[www.plantphysiol.org/cgi/doi/10.1104/pp.113.217174](http://www.plantphysiol.org/cgi/doi/10.1104/pp.113.217174)

1995). Protein profiles from seedlings with altered adventitious root formation, *argonaut1*, *sur1*, and *sur2*, identified proteins that are linked to auxin biosynthesis as candidates involved in regulation of adventitious root formation (Sorin et al., 2006).

Other studies have identified roles for auxin signaling in adventitious root formation. Plants with mutations in genes encoding auxin response factors (ARFs), which are transcription factors involved in auxin signaling, indicate that Arabidopsis ARF6, ARF8, ARF19, and ARF7 act as positive regulators (Wilmoth et al., 2005; Gutierrez et al., 2009), while ARF17 acts as a negative regulator of adventitious root development (Sorin et al., 2005). Two auxin responsive lateral organ boundary (LOB)-domain transcription factors encoded by *ADVENTITIOUS ROOTLESS1* (*ARL1*) and *CROWN ROOTLESS1* (*CRL1*) are also positive regulators of adventitious root formation in rice (*Oryza sativa*; Inukai et al., 2005; Liu et al., 2005). The gain-of-function mutant *short hypocotyl2/iaa3* has decreased adventitious root formation (Tian and Reed, 1999), while *auxin resistant3/iaa17* mutant alleles show increased formation of adventitious roots (Leyser et al., 1996).

Despite the evidence that auxin transport from the shoot apex is important in adventitious root formation (Visser et al., 1996; Guerrero et al., 1999; Díaz-Sala et al., 2002), the role of distinct auxin transport proteins in this process has not been reported. Auxin movement is mediated by influx proteins such as AUXIN RESISTANT1 (*AUX1*) and Like AUX (*LAX*), which facilitate auxin movement into cells (Marchant et al., 1999; Swarup et al., 2008), and efflux proteins such as PINFORMED (*PIN*) and ATP-BINDING CASSETTE TYPE B/P-GLYCOPROTEIN/MULTIDRUG RESISTANT (*ABCB/PGP/MDR*) proteins, which participate in auxin efflux (Gälweiler et al., 1998; Noh et al., 2001; Zazimalová et al., 2010). Defects in *AUX1*, *LAX3*, *PIN1*, and *ABCB19/PGP19/MDR1* (from here on referred to as *ABCB19*) reduce initiation and/or elongation of lateral roots (Marchant et al., 2002; Benková et al., 2003; Wu et al., 2007; Swarup et al., 2008; Lewis et al., 2011). Additionally, lateral root development has been shown to depend on complex changes in expression of *PIN* proteins prior to lateral root initiation and in developing primordia (Benková et al., 2003; Laskowski et al., 2008; Lewis et al., 2011). A recent report describes increased auxin induction of auxin influx carriers in mango cotyledons induced to form adventitious roots (Li et al., 2012). These results indicate that a distinct set of auxin transport proteins control lateral root development and suggest that similar specificity and complexity might regulate adventitious root development.

This study utilized Arabidopsis as a model to understand the role of auxin transport in adventitious root formation and to examine the molecular mechanisms by which auxin induces adventitious root formation in shoot explants. Arabidopsis seedlings grown under low-light conditions form elongated hypocotyls in which auxin transport can be measured and are optimal for root excision to induce adventitious roots. We have

examined the developmental origin and auxin response of these excision-induced roots and identified local and developmentally significant auxin-induced gene expression at the site of root excision. An array of auxin transport mutants and an *ABCB19* overexpression construct were used to demonstrate the role of *ABCB19* in adventitious root formation. Furthermore, we have examined expression of promoter and coding sequence fusions of *ABCB19* sequence to GFP and found enhanced GFP fluorescence upon root excision. These results have uncovered an underlying mechanism by which root excision alters *ABCB19*-mediated auxin transport leading to the formation of adventitious roots.

## RESULTS

### Root Excision from Arabidopsis Hypocotyls Increases Adventitious Root Formation

We asked if Arabidopsis was a feasible model to examine the mechanisms for auxin- and excision-induced adventitious root formation. Most studies aimed at identifying the role of auxin signaling in adventitious root formation in Arabidopsis hypocotyls have used intact etiolated hypocotyls (Sorin et al., 2005, 2006; Correa et al., 2012). Basipetal IAA transport is at extremely low levels in etiolated Arabidopsis hypocotyls, but levels are more amenable to study in low-light-grown hypocotyls (Rashotte et al., 2003; Liu et al., 2011), necessitating the use of alternate growth conditions for our study. As 12- to 30-d-old light-grown Arabidopsis seedlings can be induced to form adventitious roots upon root excision (Díaz-Sala et al., 2002; Correa et al., 2012), we modified these conditions for examination of younger seedlings grown in limited light to elongate hypocotyls. This allowed us to ask if we could identify the mechanisms by which excision alters auxin transport and adventitious root formation.

We germinated seedlings in low light (3–5  $\mu\text{mol m}^{-2} \text{s}^{-1}$ ) to induce hypocotyl elongation. On the fifth day after sowing, seedlings were transferred to high-light conditions (85–100  $\mu\text{mol m}^{-2} \text{s}^{-1}$ ) with and without excision of the basal half of the shoot and root system (termed root-excised hypocotyls). Intact hypocotyls form zero to one adventitious root per plant located in the middle of the hypocotyl by the eighth day after transfer to high light, while excision substantially increased the number of adventitious roots formed (Fig. 1). Excision had the advantage of reproducibly inducing adventitious roots at a position 1 to 2 mm above the site of excision, so molecular events associated with root formation could be examined at this position prior to the first detectable adventitious root.

### Adventitious Roots Induced by Excision Emerge from the Pericycle

Histological analysis suggested adventitious roots forming on intact hypocotyls initiate from pericycle

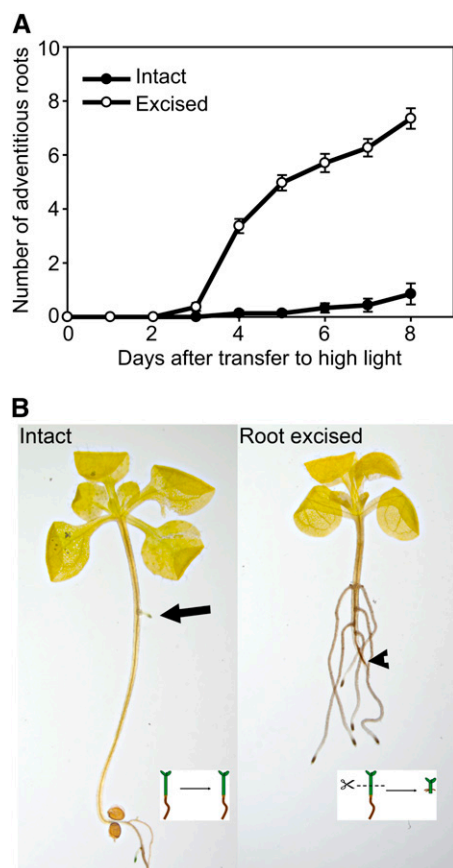


**Figure 1.** Root excision increases adventitious root formation in Arabidopsis. A, The number of adventitious roots was determined in the intact or root-excised hypocotyls ( $n = 20\text{--}30$ ). B, Adventitious root formation on intact (left) and excised (right) cleared hypocotyls is shown after 7 d. Arrow points to an adventitious root in the intact hypocotyl, and arrowhead points to site of excision. Bar = 5 mm. [See online article for color version of this figure.]

cells in Arabidopsis (Falasca and Altamura, 2003; Takahashi et al., 2003). A recent report indicated the developmental origin of adventitious roots may vary based on Arabidopsis tissue type and age used in the analysis (Correa et al., 2012). Therefore, we sought to identify the developmental origin of adventitious roots in our samples using differential interference contrast (DIC) imaging of the cleared wild type and two marker constructs, *cyclin B1* (*pCYCB1;1:GUS*) and a pericycle-expressed enhancer trap line, J0121. In cleared wild-type tissues, the sequence of adventitious root development is shown in Figure 2, with the stage of root development in each image indicated in Roman numerals corresponding to the sequence of developmental stages defined for lateral roots (Malamy and Benfey, 1997). The developing adventitious roots appear to emerge from pericycle cells in these DIC images. To define early division events, we examined the *pCYCB1;1:GUS* reporter, which is expressed in dividing cells (DiDonato et al., 2004). In basal regions of the hypocotyl, this

reporter is only expressed in adventitious root primordia (DiDonato et al., 2004), which developed close to the vascular tissue (Fig. 2B). Seedlings of the enhancer trap line J0121, which expresses GFP in pericycle cells of the hypocotyl and root (as well as epidermal cells of hypocotyls, but not roots; Laplace et al., 2005), were examined by laser scanning confocal microscopy (LSCM). These seedlings show GFP fluorescence in pericycle cells at the base of emerged adventitious roots of root-excised hypocotyls and in early-stage adventitious root primordia (Fig. 2C). The plasma membrane dye FM4-64 is largely excluded from primordia, marking them with lower fluorescence, and in the J0121:GFP reporter line, the formation of primordia from pericycle cells is evident (Fig. 2D). Thus, in low-light-grown hypocotyls, excision-induced adventitious roots of Arabidopsis, like lateral roots and adventitious roots forming on intact hypocotyls, develop from pericycle cells.

#### Transport of Auxin from the Shoot Apex Is Required for Adventitious Root Formation

We asked if Arabidopsis adventitious root formation is dependent on auxin transport under our experimental conditions, as root excision-induced adventitious roots on Arabidopsis hypocotyls show age-dependent variation in sensitivity to auxin and auxin transport inhibitors (Díaz-Sala et al., 2002; Correa et al., 2012). Treatment of root-excised hypocotyls with the IAA efflux inhibitor naphthylphthalamic acid (NPA) at  $10\ \mu\text{M}$  or removal of shoot apices prevented adventitious root formation 7 d after treatment. Additionally, the replacement of shoot apices of root-excised hypocotyls with localized IAA treatment restored adventitious root formation (Supplemental Table S1) but required high concentrations ( $100\ \mu\text{M}$ ) because of the localized application. By contrast, application of  $100\ \mu\text{M}$  NPA locally below the site of application of IAA reversed the effect of IAA. These results confirmed that auxin movement from the shoot apex is essential for adventitious rooting in our experimental system and provide background context for identifying mechanisms of auxin transport involved in excision-enhanced root formation.

In addition, we compared the effectiveness of auxin on induction of adventitious roots in intact versus root-excised hypocotyls to determine whether the response to auxin was changed by excision. Treatment of 5-d-old root-excised and intact hypocotyls with IAA increased the number of adventitious roots relative to untreated hypocotyls at concentrations ranging from 0.1 to  $25\ \mu\text{M}$  IAA (Supplemental Fig. S1). This result is consistent with increases in adventitious roots on intact Arabidopsis hypocotyls at IAA concentrations between 0.1 and  $10\ \mu\text{M}$  (Wilmoth et al., 2005) and in derooted juvenile hypocotyls (Correa et al., 2012) but differs from the report that IAA or indole-butyric acid did not stimulate adventitious rooting in mature root-excised hypocotyls (Díaz-Sala et al., 2002; Correa et al.,

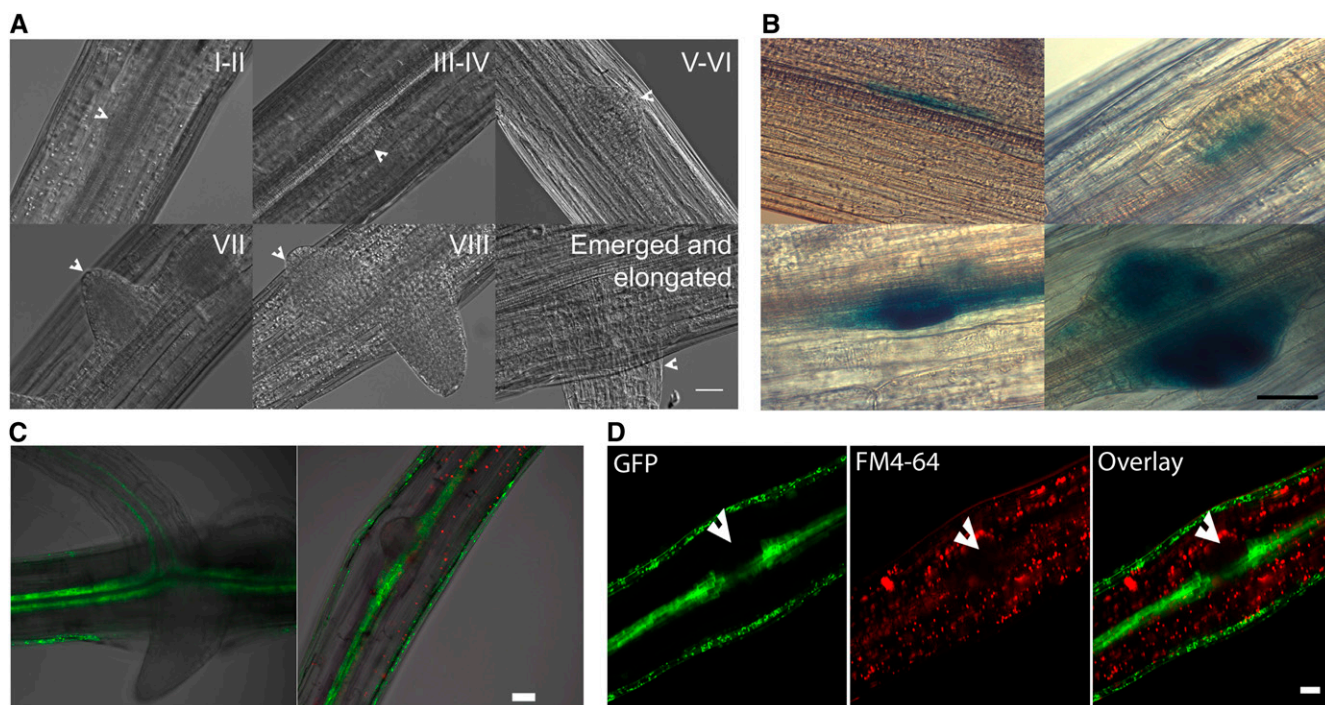


**Figure 2.** Adventitious roots emerge from pericycle tissues of the hypocotyl. DIC images of various stages of primordia development in: A, Cleared hypocotyls of the wild type at the developmental stage noted in Roman numerals; B, *AtCYCB1;1:GUS* transgenic hypocotyls; C, LSCM image of pericycle marker *J0121:GFP* in emerging adventitious roots; and D, LSCM images of pericycle marker *J0121:GFP* and FM4-64 staining in adventitious root primordia. The arrowhead notes a primordium from which most FM4-64 stain is excluded. Bars = 50  $\mu\text{m}$  (A, C, and D) and 30  $\mu\text{m}$  (B).

2012), emphasizing that developmental response to auxin varies with hypocotyl tissue age. The magnitude of induction of root formation by IAA was 1.6-fold and 13.5-fold in root-excised and intact hypocotyls, respectively. The limited response to exogenous auxin in excised hypocotyls is consistent with excision increasing auxin in the hypocotyl to a near-maximum level for root formation, resulting in limited additional response when IAA is added.

#### Excision Causes Local Increases in Auxin-Induced GUS Expression

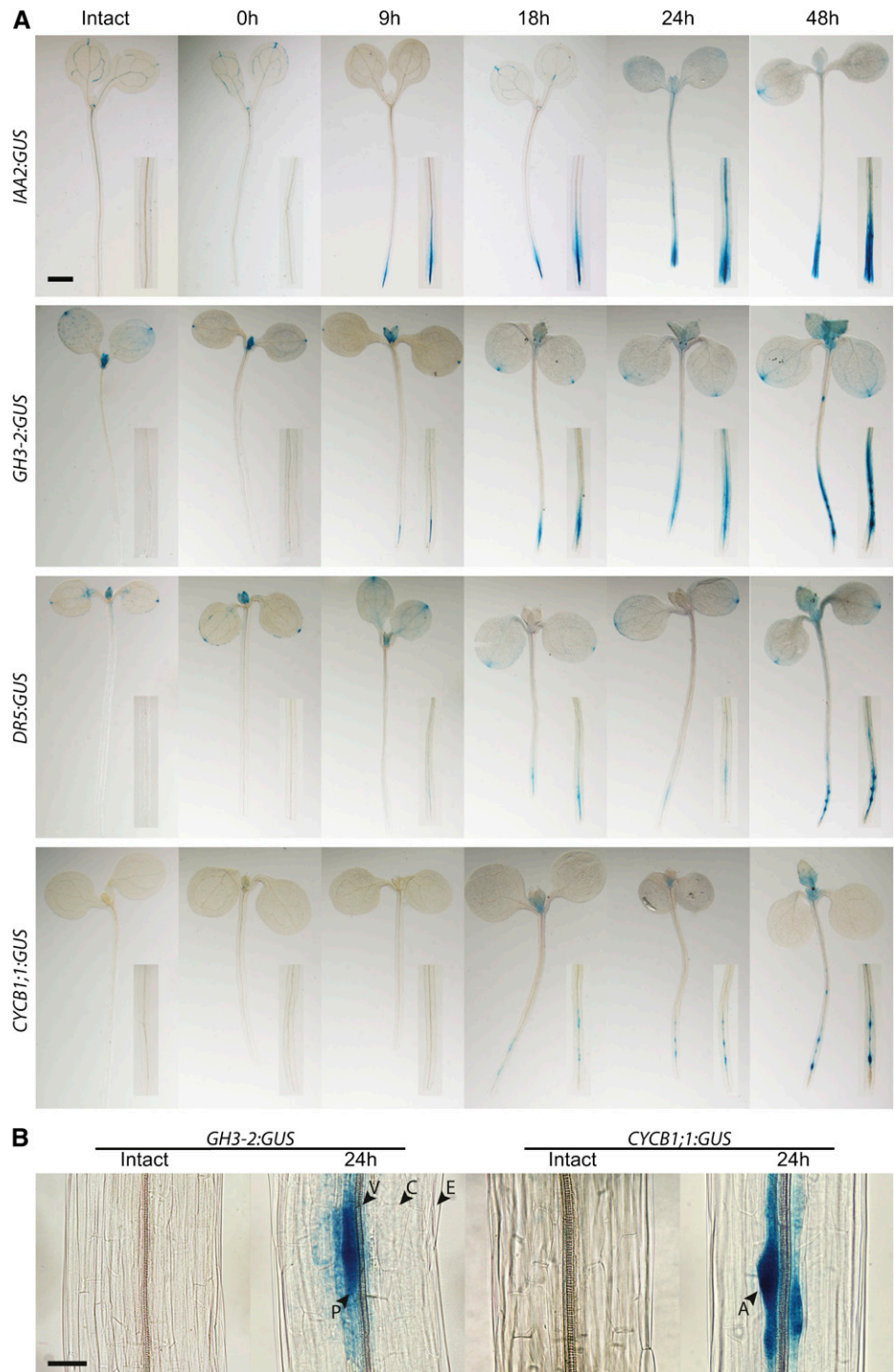
We hypothesized that the effect of excision is an increase in local auxin accumulation and signaling at the hypocotyl base, driving adventitious root formation. Hypocotyls of *Arabidopsis* plants transformed with the auxin responsive reporters *pIAA2:GUS*, *pGretchen Hagen3 (GH3)-2:GUS*, and *pDR5:GUS* were root excised, and GUS staining was initiated every hour for 9 h and at 24 and 48 h after excision (Fig. 3A). No expression was detected in these reporters in intact hypocotyls or in the hypocotyls earlier than 9 h after excision. GUS activity was detected at the base of the hypocotyl just above the site of excision and in the apices of developing adventitious roots in *pIAA2:GUS* and *pGH3-2:GUS* at 9 h after excision, while *pDR5:GUS* took longer to be detected because of its weaker signal

in this tissue (Fig. 3A). Higher magnification images of excised hypocotyls of *pGH3-2:GUS* show that GUS activity is highest in pericycle cells where adventitious root primordia are forming and is much lower in surrounding cortical cells (Fig. 3B). The presence of localized increases in expression of these auxin responsive promoter constructs above the point of excision of the hypocotyl could be due to increases in auxin synthesis, signaling, or transport. To ask if this expression occurs as a result of IAA transport, we treated *GH3-2:GUS* hypocotyls with NPA, an auxin transport inhibitor, which prevented localized *GH3-2:GUS* expression (Supplemental Fig. S2), consistent with auxin transport being required for this localized auxin-induced gene expression.

We also asked if there were changes in the level of free IAA with excision. Free IAA levels were not significantly different between intact and root-excised hypocotyls at any examined time point (Supplemental Fig. S3 and Supplemental Materials and Methods S1). Although we expected elevated free IAA after root excision to parallel the local GUS reporter increases, it is likely that free IAA only changes locally, not in the entire hypocotyl. Alternatively, because GH3-2 is an enzyme that conjugates free IAA to amino acids (Staswick et al., 2005), changes in IAA levels may be masked by elevated IAA conjugation at the hypocotyl base.

Additionally, we examined the initiation of cell division for primordium development at identical time points in

**Figure 3.** Excision increases local expression of auxin-responsive and cell division reporters in adventitious roots developing from pericycle cells. A, Intact or root-excised hypocotyls of *pIAA2:GUS*, *pGH3-2:GUS*, *pDR5:GUS*, and *AtCYCB1;1:GUS* were stained at the indicated time after excision. Insets show a 2.5× view of the hypocotyl base or the equivalent region in intact seedlings. Bar = 1 mm. B, Higher magnification images of intact or root-excised hypocotyls of *AtGH3-2:GUS* and *AtCYCB1;1:GUS* were stained 24 h after excision or in time-matched intact controls. Bar = 50 μm. Labels correspond to different cell files. P, Pericycle; V, vascular bundle; C, cortex; E, epidermis; A, adventitious root primordia.



root-excised seedlings. *pCYCB1;1:GUS* expression is detected at 18 to 24 h after root excision (Fig. 3, A and B), much later than initial detection of either auxin reporter, suggesting that local auxin accumulation precedes cell division. Higher magnification images of excised hypocotyls in this reporter line show GUS activity only in adventitious root primordia and not in surrounding cells (Fig. 3B).

#### Excision Enhances Auxin Transport, and Plants with Mutations in IAA Efflux Carriers Have Reduced Adventitious Root Formation

We examined rootward auxin transport in intact and root-excised hypocotyls. The amount of  $^3\text{H}$ -IAA, which is transported from the shoot apex and accumulates at the hypocotyl base, is increased within a little as 4 h after excision, with similar increases at 24

and 48 h after excision, with a maximal 400% increase (Fig. 4A). This is consistent with an increase in auxin transported into and remaining in the root-excised hypocotyl base, leading to local auxin accumulation, which drives adventitious root formation. The kinetics of this elevated IAA transport precede both the localized IAA accumulation detected with reporters and the initiation of adventitious roots, suggesting enhanced IAA delivery may drive this process.

As some auxin transport mutants have defects in either lateral root initiation or elongation, we asked if adventitious root formation was affected in previously characterized null alleles of auxin transport mutants *aux1-7*, *ethylene insensitive root1* (*eir1-1*, a *pin2* allele), *pin3-3*, *abcb19-1* (previously called *mdr1-1*), *pin7* (Salk 048791), and *pin1-1* (Pickett et al., 1990; Okada et al., 1991; Luschnig et al., 1998; Friml et al., 2002; Laskowski et al., 2008; Lewis et al., 2009). All mutants are in ecotype Columbia (Col-0), except *abcb19-1*, which is in ecotype Wassilewskija (Ws; Lewis et al., 2007). The adventitious rooting for each mutant is normalized relative to the appropriate wild type (Fig. 4B). Although *aux1* and *pin2* showed no significant differences in adventitious root formation, *pin3-3* and *pin7* showed slight but significant reductions relative

to the appropriate wild-type control. Of greatest significance, *abcb19-1* and *pin1-1* formed approximately 50% and 40% fewer adventitious roots than the wild type, respectively. This effect is at the level of initiation of adventitious roots, as all of the adventitious roots that initiated also emerged and elongated under these treatments, as judged by quantification of primordia at several time points after excision (data not shown). The important role of ABCB19 in this hypocotyl response is consistent with previously published microarray data showing high levels of transcripts of *ABCB19* in hypocotyls (Van Hoewyk et al., 2008; Supplemental Fig. S4), leading us to focus on the role of ABCB19 in adventitious root development.

#### ABCB19 Overexpression Increases Adventitious Root Formation and Auxin Transport

To confirm the role of *ABCB19* in adventitious root formation, we quantified adventitious root numbers in intact and root-excised hypocotyls of two *abcb19* null alleles, *abcb19-1* and *abcb19-3*, in the Ws and Col-0 backgrounds, respectively (Lewis et al., 2007), and the *ABCB19* overexpression line *p35S:ABCB19* (in Ws; Wu et al., 2010), compared with both the Ws and Col-0 wild type (Fig. 5A). The induction of adventitious roots by root excision is greater in Col-0 than Ws, largely because of lower numbers of adventitious roots formed in intact Col-0. In both *abcb19* alleles, the magnitude of the root induction by root excision is significantly reduced relative to the appropriate wild type. Intact hypocotyls of *p35S:ABCB19* formed approximately 8-fold more adventitious roots than the intact wild type. By contrast, in root-excised hypocotyls, the number of adventitious roots in the overexpression line and Ws were not significantly different. These results are consistent with excision inducing ABCB19 accumulation to levels equivalent to the overexpression lines.

To further test this hypothesis and the corollary that elevated ABCB19 protein synthesis increases hypocotyl auxin transport, we measured hypocotyl rootward (previously called basipetal)  $^3\text{H}$ -IAA transport in the *p35S:ABCB19* line and the wild type in the presence and absence of root excision. Auxin transport is not reported for *abcb19*, as the *mdr1-1* allele was previously reported to have reduced hypocotyl transport (Noh et al., 2001; Christie et al., 2011). In the wild type, excision causes enhancement of auxin transport and accumulation in the basal region of the hypocotyl, with approximately 400% increase relative to intact hypocotyls. In *p35S:ABCB19*-intact hypocotyls, transport is more than 200% of intact wild-type levels, but in excised hypocotyls, *p35S:ABCB19* shows only 120% of wild-type levels (Fig. 5B), consistent with enhanced accumulation of *ABCB19* in the wild type upon excision to roughly equivalent levels to the overexpression line.

Surprisingly, intact *abcb19-1* and *abcb19-3* hypocotyls have 4- and 1.6-fold elevated adventitious root formation relative to the wild type, respectively (Fig. 5A),

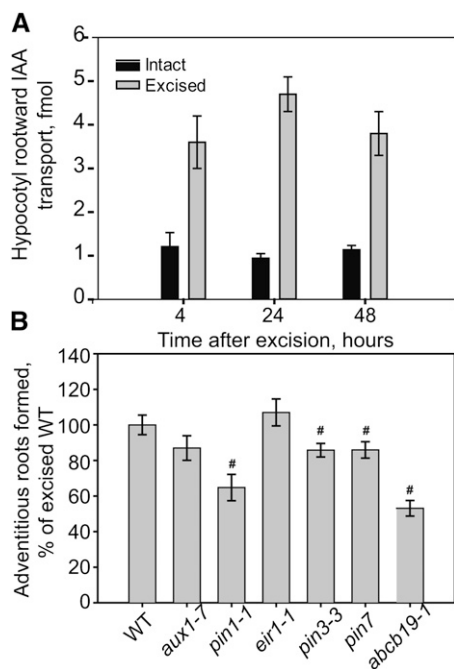


**Figure 4.** Excision induces IAA transport, and auxin transport mutants show less adventitious root formation. A, Tritiated IAA transport from the shoot apex toward the root (rootward transport) was measured in hypocotyls at the times after excision compared with intact hypocotyls. The average and  $\text{SE}$  are reported, and all samples showed significant induction by excision ( $P < 0.001$ ). B, The effect of mutations in genes encoding auxin transport proteins on adventitious roots 7 d after excision ( $n = 10\text{--}31$ ). Number sign indicates  $P \leq 0.05$  between indicated genotypes compared with the wild type (WT).

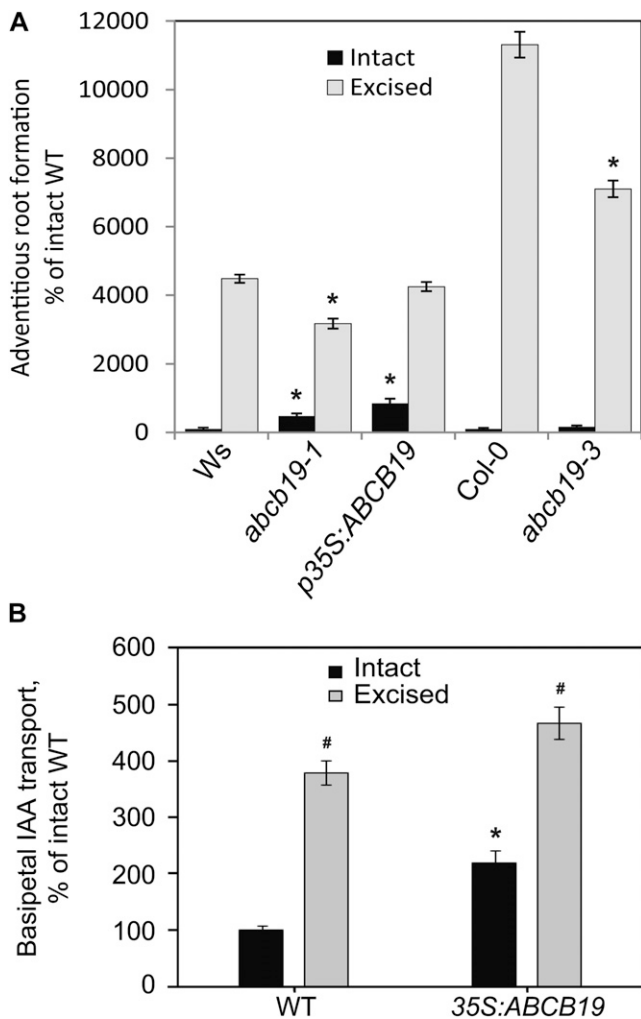


**Figure 5.** *ABCB19* expression levels are linked to excision-induced adventitious root formation and auxin transport. A, The formation of adventitious roots in intact and excised hypocotyls is reported relative to intact seedlings of the parental genotypes (Ws for *abcb19-1* and *35S:ABCB19*; Col for *abcb19-3*).  $n = 41-60$ . Asterisk indicates  $P \leq 0.05$  in excised or intact hypocotyls between genotypes. In all genotypes, excision significantly increases root formation over intact samples ( $P \leq 0.001$ ), so this is not noted on the graph. B, The effect of root excision and *p35S:ABCB19* on auxin transport 2 d after excision. The average and SE are reported. Asterisk indicates  $P \leq 0.05$  between genotypes as compared to wild type. Number sign indicates  $P \leq 0.05$  between intact and excised samples within genotypes. WT, Wild type.

contrasting with reduced formation in the root-excised mutants relative to the wild type (Fig. 4B). We hypothesize that if *ABCB19* protein is synthesized at low levels in intact hypocotyls, the high levels in roots may enhance long-distance transport from the shoot apex toward the root tip, decreasing the concentration of auxin accumulating at the hypocotyl base in the wild type. In *abcb19*, the absence of root expression would raise the levels of auxin at the base of the hypocotyl, facilitating adventitious root formation. To explore this possibility, we examined the accumulation patterns of *ABCB19* using GFP fusions.

### Excision and Overexpression Elevates *ABCB19-GFP* Fluorescence in Hypocotyls

To determine if there are changes in *ABCB19* expression and protein accumulation as a result of root excision and overexpression, we examined previously published GFP reporters *pABCB19-GFP*, *pABCB19:ABCB19-GFP*, and *p35S:ABCB19-GFP*. The fluorescence of these reporters is localized to the plasma membrane in root cells (Wu et al., 2007, 2010) and in the epidermis in the apical hook of etiolated hypocotyls (Wu et al., 2010). This construct has not been examined along the entire length of the root or hypocotyl. Intact and excised hypocotyls of these three reporters were observed 6 h after root excision, a time point chosen to examine the changes that occur before auxin accumulation, judged by the auxin-responsive reporter lines shown in Figure 3. Images were captured using LSCM tile scans, which collect multiple adjacent images, providing information on the expression patterns throughout the whole seedling (Fig. 6A). We observed expression of these reporters in the epidermis of hypocotyls, consistent with a previous examination in the hypocotyl apex (Wu et al., 2007). We also examined expression in a broader tissue context than in the previous analysis and observed bright fluorescence in the vascular tissue (Fig. 6). We have also examined the expression in individual optical slices and see that there is membrane-associated fluorescence in the pericycle layer consistent with IAA transport capacity in those cells (but at lower intensity than the adjacent vascular signal), consistent with this protein participating in auxin transport in the cells from which adventitious roots form (Supplemental Fig. S5).

In intact seedlings, the expression of the two *pABCB19*-driven constructs is stronger in the roots than in the hypocotyls (Fig. 6A). Upon root excision, both constructs show brighter fluorescence in the region directly above the point of excision, which is even more evident at higher magnification (Fig. 6B). The one interesting difference is that the transcriptional promoter construct, *pABCB19:GFP*, shows increased fluorescence in only the central cylinder, while the translational fusion, *pABCB19:ABCB19-GFP*, shows elevated expression both in the epidermis and the central cylinder.

The effect of excision on GFP fluorescence is quantified in Table I and clearly indicates that there is elevated expression of *ABCB19:GFP* in vascular tissues resulting from excision, while the absence of increased epidermal expression in the transcriptional fusion hints at additional posttranslational controls of accumulation of this protein. The *ABCB19*-driven reporter accumulates in the hypocotyl base with similar spatial characteristics to elevated IAA accumulation, as judged by *IAA2:GUS*, *GH3:GUS*, and *DR5:GUS* (Fig. 3). The excision-induced elevated expression of *pABCB19:ABCB19:GFP* occurs much more rapidly, being strongly induced at 6 h, in contrast to the detection of the auxin-induced reporters beginning at 9 h after excision. These results are consistent with *ABCB19*

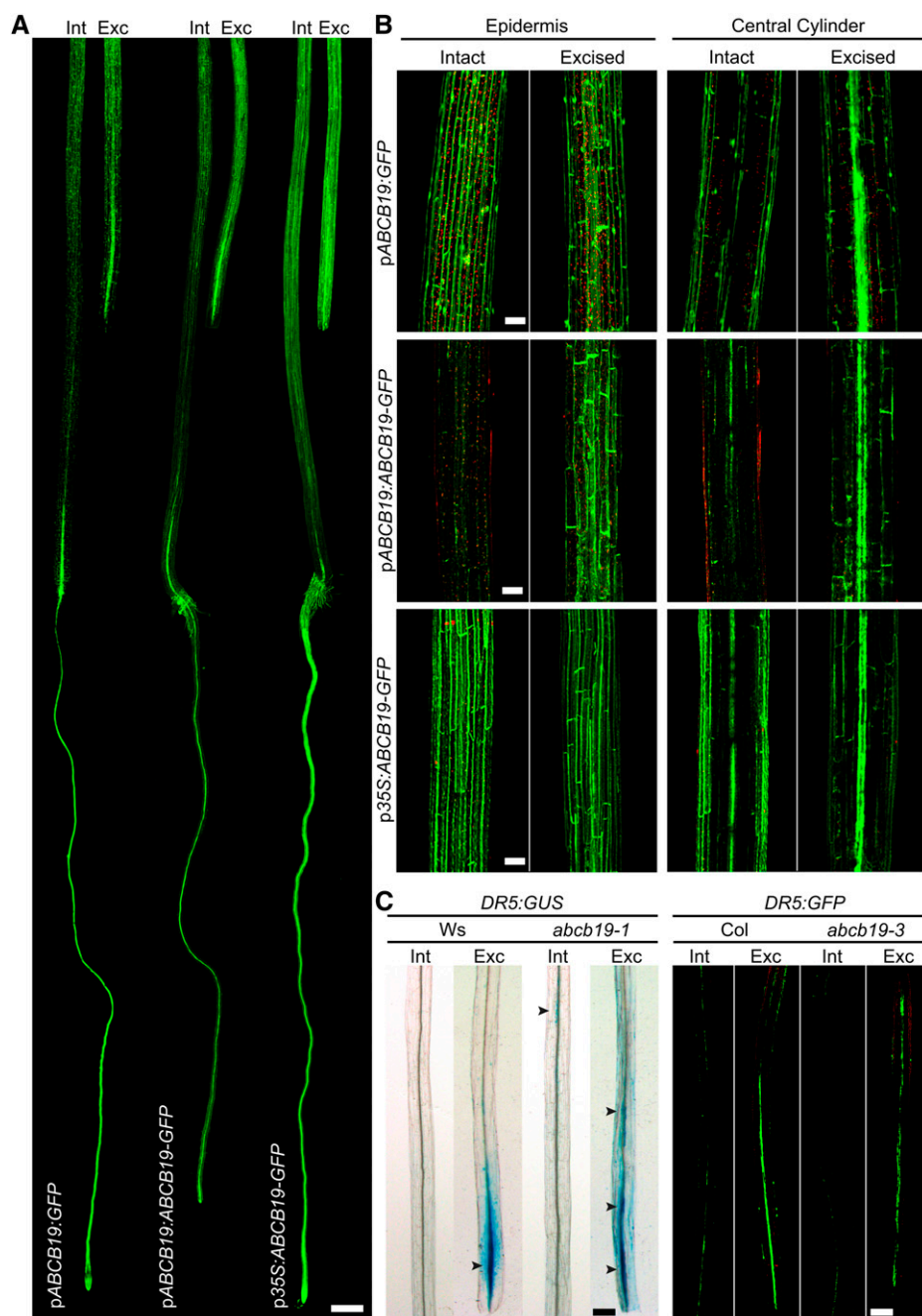


**Figure 6.** Local *ABCB19* transcription and *pABCB19:ABCB19-GFP* protein accumulations are enhanced with excision. A, LSCM tile scan images of root-excised *pABCB19:ABCB19-GFP*, *pABCB19:GFP*, and *p35S:ABCB19-GFP* taken 6 h post excision. Bar = 400  $\mu\text{m}$ . B, Comparison of intact and root-excised hypocotyls of *pABCB19:ABCB19-GFP*, *pABCB19:GFP*, and *p35S:ABCB19-GFP* examined by LSCM tile scans 6 h post excision. Bars = 100  $\mu\text{m}$ . C, Higher magnification LSCM images of *DR5:GUS* and *DR5:GFP* upon root excision in *abcb19-1* and *abcb19-3* mutant hypocotyls, respectively. Bars = 200  $\mu\text{m}$ .

driving auxin transport to create local auxin accumulation that induces adventitious root formation.

We also examined an *ABCB19* overexpression line, *35S:ABCB19:GFP*, and found that the GFP fluorescence of this construct is brighter than either endogenous promoter construct, particularly in the hypocotyl (Fig. 6, A and B). Upon excision, this expression is not substantially changed, consistent with maximal expression under the control of the 35S promoter. This effect is quantified in Table I, showing equivalent expression in the 35S promoter-driven construct to the excision-induced *pABCB19*-driven promoter. In intact hypocotyls of this overexpression line, the GFP signal

and adventitious rooting are similarly elevated relative to the wild type.

Enhanced *pABCB19*-driven GFP expression after excision is consistent with the role of *ABCB19* in mediating enhanced auxin transport resulting in auxin accumulation at the hypocotyl base, driving adventitious root formation. To test for the requirement of *ABCB19* in localized auxin accumulation, the expression patterns of two additional auxin responsive promoter-driven reporters, *pDR5:GUS* and *pDR5:GFP*, were compared in both wild-type and *abcb19* backgrounds (Fig. 6C). These reporters show enhanced expression directly above the position of root excision



**Table 1.** Excision alters GFP expression in ABCB19 transcriptional and translational fusion constructs

Quantification of intensity was performed with 12 to 21 seedlings, and values are the average  $\pm$  SE. Values for *pABCB19:ABCB19-GFP* and *35S:ABCB19-GFP* are reported as percentage of intact *pABCB19:ABCB19-GFP*. Values for *pABCB19:GFP* are reported as percentage of intact *pABCB19:GFP*.

GFP Construct	Tissue	Hypocotyl Treatment	GFP Intensity
<i>pABCB19:ABCB19-GFP</i>	Epidermis	Intact	100 $\pm$ 9
	Epidermis	Excised	247 $\pm$ 24 <sup>a</sup>
	Central cylinder	Intact	100 $\pm$ 8
	Central cylinder	Excised	284 $\pm$ 46 <sup>a</sup>
<i>35S:ABCB19-GFP</i>	Epidermis	Intact	255 $\pm$ 4 <sup>a</sup>
	Epidermis	Excised	268 $\pm$ 3 <sup>a</sup>
	Central cylinder	Intact	193 $\pm$ 13 <sup>a</sup>
	Central cylinder	Excised	288 $\pm$ 11 <sup>a</sup>
<i>pABCB19:GFP</i>	Epidermis	Intact	100 $\pm$ 6
	Epidermis	Excised	95 $\pm$ 7
	Central cylinder	Intact	100 $\pm$ 15
	Central cylinder	Excised	513 $\pm$ 19 <sup>a</sup>

<sup>a</sup>Values significantly different from intact controls used for normalized with  $P < 0.05$ .

in wild-type seedlings. By contrast, in the *abcb19-1* and *abcb19-3* null mutants, the expression of both reporters is less intense at the point of excision, with more diffuse expression along the hypocotyl, consistent with the reduced induction of adventitious root formation in this mutant upon root excision relative to the wild type (Fig. 6C). The visualization of faint *pDR5:GUS* expression in intact *abcb19-1* hypocotyls, but not wild type, is also consistent with the phenotype of this mutant, which forms more adventitious roots than the wild type in intact hypocotyls.

We have observed that root excision induces both auxin-responsive reporters and *ABCB19* reporters in the hypocotyl. It is possible that either IAA accumulation results from elevated auxin transport protein synthesis or that localized elevated IAA accumulation drives auxin transport protein synthesis. To test the possibility that auxin induces *ABCB19* accumulation, we applied 5  $\mu$ M IAA localized to the point of excision on intact and excised hypocotyls in the *pABCB19-GFP* line. We did not observe changes in GFP fluorescence in intact hypocotyls or 6 h after root excision between control and IAA treatment and only observed a slight increase in fluorescence in root-excised hypocotyls after 24 h with IAA treatment (Supplemental Fig. S6). Similarly, these IAA treatments do not restore wild-type adventitious root formation to excised hypocotyls of *abcb19-1* (data not shown). This result suggests that excision, rather than IAA accumulation, causes the induction of *ABCB19* at the hypocotyl base. It also supports our hypothesis that *ABCB19* is responsible for IAA accumulation, and not vice versa, under these conditions.

A model suggesting the mechanisms by which *ABCB19* controls adventitious root formation is illustrated in Figure 7. This model summarizes *ABCB19:GFP* fluorescence patterns (Fig. 6), auxin accumulation patterns (Fig. 3), and auxin transport (Fig. 5). This model highlights the induction of all three processes in the wild type upon root excision, with reduced

induction of all three in the *abcb19* mutant. The overexpression line has elevated *ABCB19* expression, auxin transport, and rooting in intact hypocotyls, but in excised hypocotyls, the root excision process elevates wild-type *ABCB19* and the dependent processes to levels equivalent to the overexpression construct. This model also addresses one point of complexity in our data set, the increased adventitious rooting in intact hypocotyls of two alleles of the *abcb19* mutant. Consistent with this model, the expression pattern of *pABCB19:ABCB19-GFP* in intact hypocotyls shows greater expression in the root than the hypocotyl (Fig. 6A). This suggests that in wild-type seedlings, high *ABCB19* expression in roots may act as an auxin sink, preventing the formation of auxin maxima in the hypocotyls needed for initiation of adventitious roots. In the *abcb19* mutant, the absence of this root expression may cause auxin concentration in hypocotyls to be higher than in the wild type, leading to greater numbers of adventitious roots. This model is supported by the increase in expression of the *DR5:GUS* reporter in *abcb19-1*, which suggests enhanced auxin accumulation in intact *abcb19* mutant hypocotyls (Fig. 6C). Together, these results are consistent with a mechanistic model in which root excision increases the synthesis of the *ABCB19* protein in the hypocotyl leading to elevated IAA transport and localized IAA accumulation that then drives the formation and elongation of adventitious roots.

## DISCUSSION

Lateral and adventitious roots serve important functions in plants, providing an extensively branched network that absorbs moisture and nutrients as well as providing anchorage. Despite the apparent structural similarities between adventitious and lateral roots, much less is known about the mechanisms that drive adventitious root initiation, emergence, and

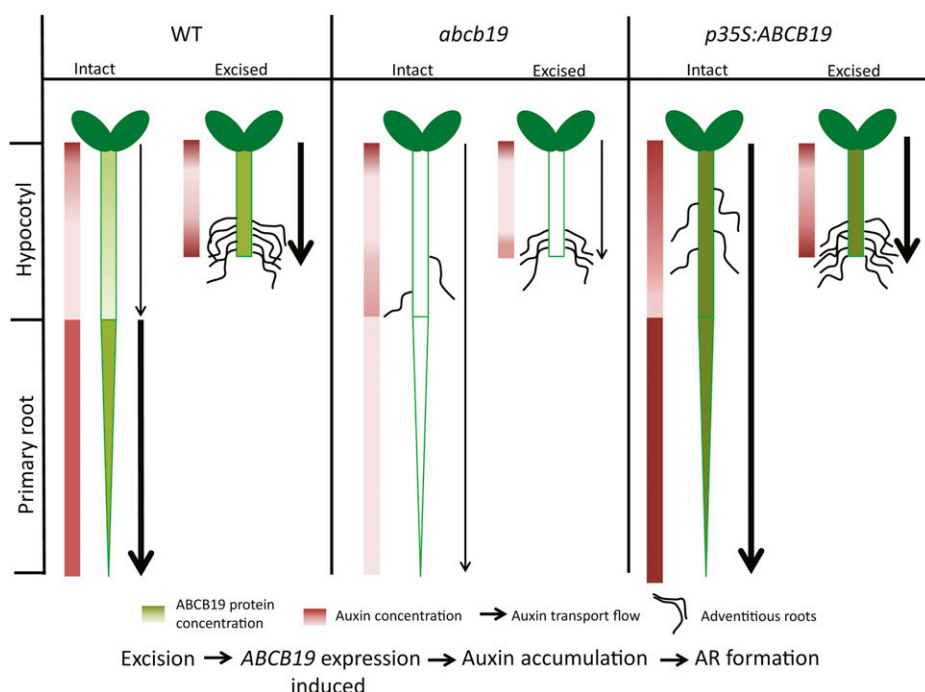


**Figure 7.** Model describing the proposed mechanisms by which excision enhances ABCB19 synthesis and auxin transport leading to localized auxin accumulation that drives adventitious root formation. The levels of ABCB19 protein are illustrated in green shading with darkness of shades proportional to expression levels, based on *ABCB19:GFP* reporter expression. The resulting levels of IAA in hypocotyls and roots are noted in shades of red to the left of each seedling, with darker red indicating higher IAA concentration. The amount of auxin transport is indicated by the width of the arrows, a thicker line denoting greater transport levels. The frequency of adventitious root formation is noted, although lateral root formation is omitted for simplicity. The flowchart at the bottom of the figure illustrates the temporal order of events occurring in the model. WT, Wild type.

elongation. The developmental sequence (Malamy and Benfey, 1997) and environmental (Malamy and Ryan, 2001) and hormonal controls (Péret et al., 2009) of lateral root formation are well studied in *Arabidopsis*, yet the low frequency of adventitious root formation (only zero to two per plant) in *Arabidopsis* has limited the studies exploring the mechanisms that drive this process (Sorin et al., 2005, 2006; Wilmoth et al., 2005; Gutierrez et al., 2009).

These experiments explored the developmental sequence and hormonal controls of excision-induced adventitious root formation in *Arabidopsis*. Previous groups had either used dark growth followed by light growth (Takahashi et al., 2003; Sorin et al., 2005, 2006; Gutierrez et al., 2009) or removal of the root from mature light-grown seedlings (Díaz-Sala et al., 2002; Correa et al., 2012) to induce adventitious root formation. We maximized adventitious root formation through a combination of these strategies. We grew seedlings under low light followed by excision of the lower half of the hypocotyl and transfer to high light. Adventitious roots form with 10-fold higher frequency under these treatments, compared with intact controls. Root excision also alters the position of adventitious root formation from the middle of intact hypocotyls to a single position localized 1 to 2 mm above the site of excision. This provides a position at which the molecular events that precede adventitious root formation can be examined. Enhanced root formation upon root excision facilitates the study of this process consistent with root excision used for vegetative propagation of horticultural and forest plant species (for review, see De Klerk et al., 1999; Abarca and Díaz-Sala, 2009). Examination of adventitious root developmental

stages allows us to conclude that increased root formation is at the level of initiation of adventitious root primordia, rather than on emergence or elongation of adventitious roots.

We have examined adventitious root development and find that excision-induced adventitious roots emerge from *Arabidopsis* hypocotyl pericycle cells, like adventitious roots forming on intact hypocotyls (Falasca and Altamura, 2003; Takahashi et al., 2003). The excision-induced adventitious roots show developmental differences from those forming on month-old light-grown seedlings (Correa et al., 2012), consistent with age-dependent differences in adventitious root induction by excision and auxin (Díaz-Sala et al., 2002; Correa et al., 2012).

Although previous studies indicated that development of adventitious root formation is controlled by a complex network of auxin-signaling proteins (Sorin et al., 2005, 2006; Wilmoth et al., 2005; Gutierrez et al., 2009), our goal was to identify the mechanisms by which auxin transport and accumulation regulates adventitious root formation. The essential role of auxin transport in initiation and development of lateral roots in *Arabidopsis* (Péret et al., 2009) and adventitious root formation in horticultural and forest species (De Klerk et al., 1999; Abarca and Díaz-Sala, 2009) has been suggested previously. Consistent with auxin transport controlling adventitious root formation, we find that removal of the auxin source at the shoot apex or treatment with the IAA efflux inhibitor NPA blocks adventitious root formation. These effects are both reversible by IAA. This finding is consistent with inhibition of adventitious rooting after NPA or 2,3,5-triiodobenzoic acid treatments in light-grown *Arabidopsis* seedlings

(Díaz-Sala et al., 2002), *Arabidopsis* inflorescence segments (Ludwig-Müller et al., 2005), etiolated carnation seedlings (Guerrero et al., 1999; Garrido et al., 2002), rice hypocotyls (Morita and Kyojuka, 2007), and pine seedlings (Díaz-Sala et al., 1996).

We find that root excision increased the flux of auxin transported from the apex to the hypocotyl base by more than 4-fold and as early as 4 h after excision, preceding any changes in adventitious root development. We detected elevated auxin-induced gene expression events directly above the point of root excision using three auxin-responsive promoter-driven GUS or GFP constructs and demonstrated that this localized gene expression was blocked by auxin transport inhibitor treatment. The increases in auxin-induced reporter expression occurred prior to the earliest cell division events leading to formation of adventitious root primordia and is blocked by treatment with auxin transport inhibitors. This finding is consistent with other auxin-dependent gene expression events that increase upon excision in tree seedlings determined by PCR and quantitative real time-PCR (Hutchison et al., 1999; Sánchez et al., 2007; Solé et al., 2008; Vielba et al., 2011) but goes beyond those prior findings to visualize the position of these localized changes using auxin-responsive reporter constructs. Together, these experiments clearly indicate an important role of auxin transport and localized auxin accumulation in excision-induced root formation.

Additionally, we explored the alternative possibility that changes in synthesis or sensitivity to auxin drives excision-induced root formation. IAA treatment stimulates adventitious root formation in intact and root-excised hypocotyls, consistent with previous reports of treatments of intact *Arabidopsis* hypocotyls (Wilmoth et al., 2005). Although the magnitude of the induction by IAA treatment is greater in intact than root-excised hypocotyls, the treatment of intact hypocotyls with high doses of IAA never leads to root formation that is equivalent to induction by root excision. These results suggest that auxin distribution, which is modified by excision, rather than the inherent sensitivity to auxin, drives the elevated response in excised hypocotyls. Additionally, we did not detect significant increases in free IAA levels in hypocotyls as a result of root excision (Supplemental Fig. S3), although we cannot rule out localized changes in free IAA or conjugates that may play a role in this process. Therefore, changes in auxin transport and resulting distribution of auxin is much more strongly implicated in enhanced root initiation in response to excision.

We used a genetic approach to identify auxin transport proteins required for enhanced adventitious root formation after root excision. Four mutants with defects in IAA efflux proteins, *pin1*, *pin3*, *pin7*, and *abcb19*, showed statistically significant reductions in adventitious root formation. Two *abcb19* mutant alleles had the greatest reductions in excision-induced root formation, suggesting that ABCB19 may transport auxin required for adventitious root initiation. Overexpression lines of

*ABCB19* had enhanced auxin transport and adventitious root initiation in intact hypocotyls, consistent with this hypothesis. Although additional proteins likely participate in the regulation of adventitious root formation, this result strongly indicates a role for ABCB19 in adventitious root formation.

To further understand the mechanism of enhanced IAA transport after root excision, we examined the GFP fluorescence of *ABCB19* transcriptional and translational fusions under the control of endogenous and 35S promoters. These reporters are expressed in both epidermal tissues and vascular and pericycle cells, with the later localization linked to controlling auxin delivery to developing lateral root primordia. GFP fluorescence of *ABCB19* transcriptional and translational fusions increases after root excision in the region above the point of excision, with similar increases in the central cylinder in both fusions. The increases in fluorescence in the epidermal layer are restricted to the *pABCB19:ABCB19-GFP* construct, suggesting that root excision may also affect ABCB19 protein abundance via a posttranscriptional mechanism. This finding is intriguing in light of the recent report that ABCB19 is phosphorylated by phototropin1 as a posttranslational regulation to modulate ABCB19 auxin transport activity (Christie et al., 2011).

We also determined that localized exogenous IAA did not significantly increase *pABCB19:GFP* reporter levels in intact or root-excised hypocotyls. This result suggests excision induces *ABCB19* expression, leading to IAA accumulation at the hypocotyl base, rather than the converse. We quantified transcript levels of *ABCB19* in intact and root-excised hypocotyls using quantitative reverse transcription-PCR but found no difference in expression levels (data not shown). The lack of detectable transcript changes is likely due to the local and tissue-specific changes in *ABCB19* expression that limit detection in whole seedlings. The *ABCB19* overexpression construct also provides insight into this regulation. *p35S:ABCB19-GFP* exhibited greater fluorescence in the hypocotyl and root in intact seedlings relative to the endogenous promoter-driven reporter. By contrast, in root-excised hypocotyls, the fluorescence of this *p35S*-driven construct is equivalent to the endogenous promoter-driven *ABCB19* construct, consistent with the induction of ABCB19 synthesis to the levels of the overexpression line, upon root excision. These expression changes are directly correlated with elevated adventitious root formation in either root-excised wild-type or overexpression lines and the absence of cumulative induction in root-excised overexpression lines.

Surprisingly, intact seedlings of two alleles of *abcb19* formed more adventitious roots than the intact wild type, with either 4- or 1.6-fold increases. The detailed examination of expression of the *pABCB19*-driven GFP fusion constructs provided insight into the initially surprising adventitious root phenotype. *pABCB19*-driven transcriptional and translational fusions to GFP show strong expression in the root and weak expression in intact hypocotyls. Elevated rooting in intact *abcb19* seedlings can be explained by the higher levels

of expression of *ABCB19* seen in wild-type roots that act as a sink, thereby reducing auxin accumulation in wild-type hypocotyl and the absence of this sink enhancing root formation in the mutant. Consistent with this hypothesis, the auxin-responsive reporter *DR5:GUS* was expressed in intact *abcb19* hypocotyls but not in the wild type, consistent with enhanced auxin accumulation in intact hypocotyls of this mutant.

These findings suggest mechanisms by which root excision induces adventitious root formation. The model in Figure 7 summarizes the proposed mechanisms by which the events described here are linked. In wild-type plants, root excision enhances transport of auxin and localized accumulation of auxin at the site of excision driving localized initiation and emergence of adventitious roots. In *abcb19* mutant plants, intact hypocotyls form more adventitious roots, likely through the reduction in auxin transport away from the hypocotyl into the root. The *abcb19* mutant also shows less induction of adventitious root initiation due to reduced hypocotyl IAA transport due to a lack of ABCB19 protein. In plants in which overexpression constructs lead to higher levels of ABCB19, there are more adventitious roots formed on the hypocotyl, as the expression of this protein is most elevated in the hypocotyl. By contrast, excision does not elevate *ABCB19* expression further, so the number of adventitious roots on root-excised wild-type and *ABCB19* overexpression lines are similar. Together, these results provide a logical model in which excision drives synthesis of the ABCB19 auxin transport protein leading to elevated auxin transport and localized auxin levels that drive initiation of adventitious roots.

## MATERIALS AND METHODS

### Plant Materials and Chemicals

Col-0 and Ws ecotypes were used in this study. Seeds were provided by Edgar Spalding (*abcb19* null alleles; *mdr1-1* and *mdr1-3* in the Ws and Col-0 backgrounds [Lewis et al., 2007]; *pABCB19:GFP*, *pABCB19:ABCB19-GFP*, and *pDR5:GUS* in *mdr1-1* [Wu et al., 2007]; and *p35S-ABCB19* and *p35S:ABCB19-GFP* [Wu et al., 2010]), Gretchen Hagen (*AtGH3-2:GUS* line 19), Marta Laskowski (*pin3* and *pin7*; Laskowski et al., 2008), and Malcolm Bennett (*IAA2:GUS* and *aux1*; Swarup et al., 2007). All other mutants were received from the Arabidopsis Biological Resource Center, and all are null alleles.

<sup>3</sup>H-IAA (24 and 20 Ci mmol<sup>-1</sup>) was purchased from Amersham or American Radiolabeled Chemicals. NPA was purchased from Chemical Services. RNA isolation was done using Qiagen plant RNeasy kit. Reagents used for ribonuclease treatment and complementary DNA synthesis were purchased from Invitrogen. Reagents for DNase treatment were purchased from Promega. SYBR green reagent was purchased from Applied Biosystems. All other chemicals were purchased from Sigma.

### Plant Growth Conditions and Quantification of Adventitious Roots

Seeds were sterilized and placed on medium containing 0.8% (w/v) Type M agar (A-4800, Sigma), 1× Murashige and Skoog nutrients (macro and micro salts), vitamins (1 μg mL<sup>-1</sup> thiamine, 1 μg mL<sup>-1</sup> pyridoxine HCl, and 0.5 μg mL<sup>-1</sup> nicotinic acid), 1.5% (w/v) Suc, and 0.05% (w/v) MES, with pH adjusted to 5.8 with 1N KOH before autoclaving. Seedlings were grown in vertical orientation with constant light at 3 to 5 μmol m<sup>-2</sup> s<sup>-2</sup> for 5 d to induce hypocotyl

elongation. These seedlings were left intact or roots, and the hypocotyl base was excised using Neuro clipper scissors (Fine Science Tools) at a position 5 to 7.5 mm from the shoot apex, followed by growth for 7 d under constant 85 to 100 μmol m<sup>-2</sup> s<sup>-1</sup> light (at approximately 25°C). Adventitious roots were quantified on the seventh day unless otherwise indicated using a dissecting microscope, including only roots formed on the hypocotyl above, but not including, the root-shoot junction. DIC images of developing adventitious roots were taken using a Zeiss Axio Observer inverted microscope.

### GUS Staining

*AtGH3-2:GUS*, *AtCYCB1;1:GUS*, *AHAA2:GUS*, and *DR5:GUS* transgenic seedlings were incubated in GUS substrate (100 mM sodium phosphate buffer, 0.5% (v/v) Triton X, 2 mM X-gluc salt, 0.5 mM ferricyanide, and 0.5 mM ferrocyanide) at 37°C for 24 h. Samples were washed with 100 mM sodium phosphate buffer, pH 7, and stored in 95% ethanol. The samples were fixed in 10% (v/v) formaldehyde, 5% (v/v) acetic acid, and 50% (v/v) ethanol overnight at 4°C and cleared using chloral hydrate:glycerol:water solution (8:1:2, w/v/v) at room temperature and mounted in 95% (v/v) ethanol. GUS staining was visualized by a Leica MZ16FA epifluorescent stereomicroscope.

### Applications of IAA and NPA

Stocks were prepared at 10 mM in ethanol and dimethyl sulfoxide and added to cooled medium at indicated concentrations. Experiments involving IAA treatments were placed under fluorescent lights with yellow filters (Stasinopoulos and Hangarter, 1990) to prevent white light-induced degradation of IAA. For local applications, compounds were added in 1% (w/v) agar in 5 mM MES, pH 5.5, at 50°C and placed in scintillation vials. One-millimeter agar cylinders were obtained by using sterile plastic transfer pipettes to cut cores from the solidified agar. Localized application of NPA was done as a second agar cylinder below the agar cylinder containing IAA. Observations on position and number of emerged adventitious roots were performed after 7 d using a dissecting microscope.

### LSCM

GFP fluorescence was observed in water-mounted samples using a Zeiss LSM710 fluorescence laser scanning confocal microscope using either the GFP channel (*J0121:GFP*) at 494 to 649 nm or λ scanning (*ABCB19-GFP* lines). GFP and chloroplast signals were separated using two channels, 493 to 556 and 637 to 721 nm, respectively. Quantification of GFP signals were performed using linear profiles through the longitudinal sides of the cells using Zeiss Zen software. Tile scanning of hypocotyls was performed using Zen software. All images for each genotype within an experiment were captured under identical laser, gain, and pinhole settings.

### Auxin Transport

Hypocotyl auxin transport measurements were performed by modifying a previously published method (Lewis and Muday, 2009). Five-day-old low-light-grown seedlings, either intact or excised, were transferred to control plates, and their shoot apices were removed. Roots were excised 48 h prior to assay. An agar cylinder or agar droplet with <sup>3</sup>H-IAA (100 nM) was applied at the shoot end and incubated in the dark for 3 h. Three-millimeter sections were removed from the basal end from the excised hypocotyls (and at a similar position from the apex in the intact hypocotyls). Transport occurred for 3 h, and radioactivity was quantified by scintillation counting.

Methods for quantification of free IAA are provided in Supplemental Materials and Methods S1.

Sequence data from this article can be found in the GenBank/EMBL data libraries under accession numbers ABCB19 (AT3G28860), AUX1 (AT2G38120), IAA2 (AT3G23030), PIN1 (AT1G73590), PIN2 (AT5G57090), PIN3 (AT1G70940), and PIN7 (AT1G23080).

### Supplemental Data

The following materials are available in the online version of this article.

**Supplemental Figure S1.** The effect of IAA on adventitious root formation and IAA transport in hypocotyls.

**Supplemental Figure S2.** Hypocotyls of *AtGH3-2:GUS* transgenic seedlings were stained prior to excision, at the time of excision, and at 24 h after root excision with or without 10  $\mu$ M NPA added.

**Supplemental Figure S3.** Free IAA levels were quantified using IAA extraction followed by detection using gas chromatography-mass spectrometry.

**Supplemental Figure S4.** Transcript abundance of genes encoding IAA signaling and IAA transport proteins from a previously published microarray data set using hypocotyl tissues (Van Hoewyk et al., 2008).

**Supplemental Figure S5.** *pABC19:GFP* fluorescence is found in vascular and pericycle cells.

**Supplemental Figure S6.** The effect of IAA on GFP fluorescence in the *pABC19:GFP* line.

**Supplemental Table S1.** The role of shoot derived auxin in adventitious root formation.

**Supplemental Materials and Methods S1.** The method for free IAA measurement is outlined (Barkawi et al. 2008).

## ACKNOWLEDGMENTS

We thank Sangeeta Negi, Daniel Lewis, and Hanya Chrispeels for thoughtful comments, Gretchen Hagen, Malcolm Bennett, Marta Laskowski, and Edgar Spalding for sharing mutant or transgenic *Arabidopsis* seeds, Anita McCauley for microscopy assistance, and Jerry Cohen and Xing Liu for assistance in performing the free IAA measurements.

Received March 1, 2013; accepted May 3, 2013; published May 15, 2013.

## LITERATURE CITED

- Abarca D, Díaz-Sala C (2009) Reprogramming adult cells during organ regeneration in forest species. *Plant Signal Behav* 4: 793–795
- Barkawi LS, Tam YY, Tillman JA, Pederson B, Calio J, Al-Amier H, Emerick M, Normanly J, Cohen JD (2008) A high-throughput method for the quantitative analysis of indole-3-acetic acid and other auxins from plant tissue. *Anal Biochem* 372: 177–188
- Benková E, Michniewicz M, Sauer M, Teichmann T, Seifertová D, Jürgens G, Friml J (2003) Local, efflux-dependent auxin gradients as a common module for plant organ formation. *Cell* 115: 591–602
- Boerjan W, Cervera MT, Delarue M, Beeckman T, Dewitte W, Bellini C, Caboche M, Van Onckelen H, Van Montagu M, Inzé D (1995) *Super-root*, a recessive mutation in *Arabidopsis*, confers auxin overproduction. *Plant Cell* 7: 1405–1419
- Celenza JL Jr, Grisafi PL, Fink GR (1995) A pathway for lateral root formation in *Arabidopsis thaliana*. *Genes Dev* 9: 2131–2142
- Christie JM, Yang H, Richter GL, Sullivan S, Thomson CE, Lin J, Titapiwatanakun B, Ennis M, Kaiserli E, Lee OR, et al (2011) *phot1* inhibition of ABCB19 primes lateral auxin fluxes in the shoot apex required for phototropism. *PLoS Biol* 9: e1001076
- Correa Lda R, Troleis J, Mastroberti AA, Mariath JE, Fett-Neto AG (2012) Distinct modes of adventitious rooting in *Arabidopsis thaliana*. *Plant Biol (Stuttg)* 14: 100–109
- De Klerk G-J, Van Der Krieken W, De Jong JC (1999) The formation of adventitious roots: new concepts, new possibilities. *In Vitro Cell Dev Biol-Plant* 35: 481–490
- Díaz-Sala C, Garrido G, Sabater B (2002) Age-related loss of rooting capability in *Arabidopsis thaliana* and its reversal by peptides containing the Arg-Gly-Asp (RGD) motif. *Physiol Plant* 114: 601–607
- Díaz-Sala C, Hutchison K, Goldfarb B, Greenwood M (1996) Maturation-related loss in rooting competence by loblolly pine stem cutting: the role of auxin transport, metabolism and tissue sensitivity. *Physiol Plant* 97: 481–490
- DiDonato RJ, Arbuckle E, Buker S, Sheets J, Tobar J, Totong R, Grisafi P, Fink GR, Celenza JL (2004) *Arabidopsis ALF4* encodes a nuclear-localized protein required for lateral root formation. *Plant J* 37: 340–353
- Falasca G, Altamura M (2003) Histological analysis of adventitious rooting in *Arabidopsis thaliana* (L.) Heynh seedlings. *Plant Biosyst* 137: 265–274
- Friml J, Wiśniewska J, Benková E, Mendgen K, Palme K (2002) Lateral relocation of auxin efflux regulator PIN3 mediates tropism in *Arabidopsis*. *Nature* 415: 806–809
- Gälweiler L, Guan C, Müller A, Wisman E, Mendgen K, Yephremov A, Palme K (1998) Regulation of polar auxin transport by *AtPIN1* in *Arabidopsis* vascular tissue. *Science* 282: 2226–2230
- Garrido G, Ramón Guerrero J, Angel Cano E, Acosta M, Sánchez-Bravo J (2002) Origin and basipetal transport of the IAA responsible for rooting of carnation cuttings. *Physiol Plant* 114: 303–312
- Guerrero JR, Garrido G, Acosta M, Sánchez-Bravo J (1999) Influence of 2,3,5-triiodobenzoic acid and 1-N-naphthylphthalamic acid on indoleacetic acid transport in carnation cuttings: relationship with rooting. *J Plant Growth Regul* 18: 183–190
- Gutierrez L, Russell JD, Pacurar DI, Schwambach J, Pacurar M, Bellini C (2009) Phenotypic plasticity of adventitious rooting in *Arabidopsis* is controlled by complex regulation of *AUXIN RESPONSE FACTOR* transcripts and microRNA abundance. *Plant Cell* 21: 3119–3132
- Hutchison KW, Singer PB, McInnis S, Diaz-Sala C, Greenwood MS (1999) Expansins are conserved in conifers and expressed in hypocotyls in response to exogenous auxin. *Plant Physiol* 120: 827–832
- Inukai Y, Sakamoto T, Ueguchi-Tanaka M, Shibata Y, Gomi K, Umemura I, Hasegawa Y, Ashikari M, Kitano H, Matsuoka M (2005) *Crown rootless1*, which is essential for crown root formation in rice, is a target of an *AUXIN RESPONSE FACTOR* in auxin signaling. *Plant Cell* 17: 1387–1396
- Laplace L, Parizot B, Baker A, Ricaud L, Martinière A, Auguy F, Franche C, Nussaume L, Bogusz D, Haseloff J (2005) *GAL4-GFP* enhancer trap lines for genetic manipulation of lateral root development in *Arabidopsis thaliana*. *J Exp Bot* 56: 2433–2442
- Laskowski M, Grieneisen VA, Hofhuis H, Hove CA, Hogeweg P, Marée AF, Scheres B (2008) Root system architecture from coupling cell shape to auxin transport. *PLoS Biol* 6: e307
- Lewis DR, Miller ND, Splitt BL, Wu G, Spalding EP (2007) Separating the roles of acropetal and basipetal auxin transport on gravitropism with mutations in two *Arabidopsis* multidrug resistance-like ABC transporter genes. *Plant Cell* 19: 1838–1850
- Lewis DR, Muday GK (2009) Measurement of auxin transport in *Arabidopsis thaliana*. *Nat Protoc* 4: 437–451
- Lewis DR, Negi S, Sukumar P, Muday GK (2011) Ethylene inhibits lateral root development, increases IAA transport and expression of PIN3 and PIN7 auxin efflux carriers. *Development* 138: 3485–3495
- Lewis DR, Wu G, Ljung K, Spalding EP (2009) Auxin transport into cotyledons and cotyledon growth depend similarly on the ABCB19 Multidrug Resistance-like transporter. *Plant J* 60: 91–101
- Leyser HM, Pickett FB, Dharmasiri S, Estelle M (1996) Mutations in the *AXR3* gene of *Arabidopsis* result in altered auxin response including ectopic expression from the *SAUR-AC1* promoter. *Plant J* 10: 403–413
- Li S, Xue L, Xu S, Fieng H, An L (2009) Mediators, genes, and signaling in adventitious rooting. *Bot Rev* 75: 230–247
- Li Y-H, Zou MH, Feng B-H, Huang X, Zhang Z, Sun G-M (2012) Molecular cloning and characterization of the genes encoding an auxin efflux carrier and the auxin influx carriers associated with the adventitious root formation in mango (*Mangifera indica* L.) cotyledon segments. *Plant Physiol Biochem* 55: 33–42
- Liu H, Wang S, Yu X, Yu J, He X, Zhang S, Shou H, Wu P (2005) ARL1, a LOB-domain protein required for adventitious root formation in rice. *Plant J* 43: 47–56
- Liu X, Cohen JD, Gardner G (2011) Low-fluence red light increases the transport and biosynthesis of auxin. *Plant Physiol* 157: 891–904
- Ludwig-Müller J, Vertocnik A, Town CD (2005) Analysis of indole-3-butyric acid-induced adventitious root formation on *Arabidopsis* stem segments. *J Exp Bot* 56: 2095–2105
- Luschnig C, Gaxiola RA, Grisafi P, Fink GR (1998) EIR1, a root-specific protein involved in auxin transport, is required for gravitropism in *Arabidopsis thaliana*. *Genes Dev* 12: 2175–2187
- Malamy JE, Benfey PN (1997) Organization and cell differentiation in lateral roots of *Arabidopsis thaliana*. *Development* 124: 33–44
- Malamy JE, Ryan KS (2001) Environmental regulation of lateral root initiation in *Arabidopsis*. *Plant Physiol* 127: 899–909
- Marchant A, Bhalerao R, Casimiro I, Eklöf J, Casero PJ, Bennett M, Sandberg G (2002) AUX1 promotes lateral root formation by facilitating indole-3-acetic acid distribution between sink and source tissues in the *Arabidopsis* seedling. *Plant Cell* 14: 589–597

- Marchant A, Kargul J, May ST, Muller P, Delbarre A, Perrot-Rechenmann C, Bennett MJ (1999) *AUX1* regulates root gravitropism in *Arabidopsis* by facilitating auxin uptake within root apical tissues. *EMBO J* **18**: 2066–2073
- Morita Y, Kyoizuka J (2007) Characterization of *OsPID*, the rice ortholog of *PINOID*, and its possible involvement in the control of polar auxin transport. *Plant Cell Physiol* **48**: 540–549
- Noh B, Murphy AS, Spalding EP (2001) *Multidrug resistance*-like genes of *Arabidopsis* required for auxin transport and auxin-mediated development. *Plant Cell* **13**: 2441–2454
- Okada K, Ueda J, Komaki MK, Bell CJ, Shimura Y (1991) Requirement of the auxin polar transport system in early stages of *Arabidopsis* floral bud formation. *Plant Cell* **3**: 677–684
- Péret B, De Rybel B, Casimiro I, Benková E, Swarup R, Laplaze L, Beeckman T, Bennett MJ (2009) *Arabidopsis* lateral root development: an emerging story. *Trends Plant Sci* **14**: 399–408
- Pickett FB, Wilson AK, Estelle M (1990) The *aux1* mutation of *Arabidopsis* confers both auxin and ethylene resistance. *Plant Physiol* **94**: 1462–1466
- Rashotte AM, Poupart J, Waddell CS, Muday GK (2003) Transport of the two natural auxins, indole-3-butyric acid and indole-3-acetic acid, in *Arabidopsis*. *Plant Physiol* **133**: 761–772
- Sánchez C, Vielba JM, Ferro E, Covelo G, Solé A, Abarca D, de Mier BS, Díaz-Sala C (2007) Two *SCARECROW-LIKE* genes are induced in response to exogenous auxin in rooting-competent cuttings of distantly related forest species. *Tree Physiol* **27**: 1459–1470
- Solé A, Sánchez C, Vielba JM, Valladares S, Abarca D, Díaz-Sala C (2008) Characterization and expression of a *Pinus radiata* putative ortholog to the *Arabidopsis* *SHORT-ROOT* gene. *Tree Physiol* **28**: 1629–1639
- Sorin C, Bussell JD, Camus I, Ljung K, Kowalczyk M, Geiss G, McKhann H, Garcion C, Vaucheret H, Sandberg G, et al (2005) Auxin and light control of adventitious rooting in *Arabidopsis* require ARGONAUTE1. *Plant Cell* **17**: 1343–1359
- Sorin C, Negroni L, Balliau T, Corti H, Jacquemot MP, Davanture M, Sandberg G, Zivy M, Bellini C (2006) Proteomic analysis of different mutant genotypes of *Arabidopsis* led to the identification of 11 proteins correlating with adventitious root development. *Plant Physiol* **140**: 349–364
- Stasinopoulos TC, Hangarter RP (1990) Preventing photochemistry in culture media by long-pass light filters alters growth of cultured tissues. *Plant Physiol* **93**: 1365–1369
- Staswick PE, Serban B, Rowe M, Tiryaki I, Maldonado MT, Maldonado MC, Suza W (2005) Characterization of an *Arabidopsis* enzyme family that conjugates amino acids to indole-3-acetic acid. *Plant Cell* **17**: 616–627
- Swarup K, Benková E, Swarup R, Casimiro I, Péret B, Yang Y, Parry G, Nielsen E, De Smet I, Vanneste S, et al (2008) The auxin influx carrier LAX3 promotes lateral root emergence. *Nat Cell Biol* **10**: 946–954
- Swarup R, Perry P, Hagenbeek D, Van Der Straeten D, Beemster GT, Sandberg G, Bhalerao R, Ljung K, Bennett MJ (2007) Ethylene upregulates auxin biosynthesis in *Arabidopsis* seedlings to enhance inhibition of root cell elongation. *Plant Cell* **19**: 2186–2196
- Takahashi F, Sato-Nara K, Kobayashi K, Suzuki M, Suzuki H (2003) Sugar-induced adventitious roots in *Arabidopsis* seedlings. *J Plant Res* **116**: 83–91
- Tian Q, Reed JW (1999) Control of auxin-regulated root development by the *Arabidopsis thaliana* *SHY2/IAA3* gene. *Development* **126**: 711–721
- Van Hoewyk D, Takahashi H, Inoue E, Hess A, Tamaoki M, Pilon-Smits EA (2008) Transcriptome analyses give insights into selenium-stress responses and selenium tolerance mechanisms in *Arabidopsis*. *Physiol Plant* **132**: 236–253
- Vielba JM, Díaz-Sala C, Ferro E, Rico S, Lamprecht M, Abarca D, Ballester A, Sánchez C (2011) *CsSCL1* is differentially regulated upon maturation in chestnut microshoots and is specifically expressed in rooting-competent cells. *Tree Physiol* **31**: 1152–1160
- Visser E, Cohen JD, Barendse G, Blom C, Voesenek L (1996) An ethylene-mediated increase in sensitivity to auxin induces adventitious root formation in flooded *rumex palustris* Sm. *Plant Physiol* **112**: 1687–1692
- Wilmoth JC, Wang S, Tiwari SB, Joshi AD, Hagen G, Guilfoyle TJ, Alonso JM, Ecker JR, Reed JW (2005) NPH4/ARF7 and ARF19 promote leaf expansion and auxin-induced lateral root formation. *Plant J* **43**: 118–130
- Wu G, Cameron JN, Ljung K, Spalding EP (2010) A role for ABCB19-mediated polar auxin transport in seedling photomorphogenesis mediated by cryptochrome 1 and phytochrome B. *Plant J* **62**: 179–191
- Wu G, Lewis DR, Spalding EP (2007) Mutations in *Arabidopsis* multidrug resistance-like ABC transporters separate the roles of acropetal and basipetal auxin transport in lateral root development. *Plant Cell* **19**: 1826–1837
- Zazimalová E, Murphy AS, Yang HB, Hoyerová K, Hosek P (2010) Auxin transporters—why so many? *Cold Spring Harb Perspect Biol* **2**: a001552